2025, Vol. 5, No. 2, pp. 136-167

Journal of Anomalous Experience and Cognition (JAEX)

Investigating the Brain Processes Underlying an Unusual Visual Experience: A Case Study[1]

Cedric Cannard,[a] Cassandra Vieten,[b] Garret Yount,[a] Mateo Vega,[a]
Fadi Kayale,[a, c] Arnaud Delorme[a, b, d]

a) Institute of Noetic Sciences, b) University of California San Diego,
c) University of Toronto, d) Université Paul Sabatier

Abstract: *Background*. This case study investigated the neural correlates of an unusual visual experience in which an individual constantly perceives highly detailed holographic images overlaid on his visual field and can modulate them to an extent. We named this experience *Upsight*. Our aim was to assess how the phenomenon may relate or differ from visual mental imagery (VMI such as hyperphantasia), imagination, or visual hallucinations (e.g., Charles Bonnet Syndrome). *Method*: EEG (64-channels) data were collected while the participant alternated between 30-second trials of *Upsight* and visual mental imagery (VMI) conditions (200 trials each). We conducted power spectral density (scalp and source levels) as well as source functional connectivity (FC) analyses, as well as robust statistics to test the null hypothesis of an absence of a difference (nonparametric statistics and spatiotemporal cluster corrections). *Results*: Scalp results revealed that, relative to VMI, the *Upsight* experience was characterized by strong alpha and delta power decreases (widespread with a peak in posterior regions), and gamma power increase (29-45 Hz) in the right frontal and left posterior regions, supporting increased engagement of cognitive and visual processes. Similarly, after source localization, we observed a strong decrease in both spectral power and FC in the alpha frequency band, in brain areas involved in visual processing, spatial orientation, and sensory integration, reflecting increased cortical activation of these areas and brain networks. *Conclusions*: *Upsight* involves heightened engagement and processing in visual and cognitive networks relative to VMI. We discuss the phenomenology and results in relation to VMI, imagination, and visual hallucinations.

1 Address correspondence to: Garret Yount, Ph., D., Institute of Noetic Sciences, 7250 Redwood Blvd., Suite 208, Novato, CA, USA, gyount@noetic.org

https://doi.org/10.311356/jaex.25894

Keywords: EEG, vision, perception, *Upsight*, visual mental imagery (VMI), source localization, functional connectivity, anomalous experience

Highlights

- This case study explored *Upsight*, a unique visual phenomenon with continuous and vivid holographic images overlaid on the visual field.
- EEG analyses showed reduced alpha power and increased high-frequency activity during *Upsight* compared to visual mental imagery (VMI), indicating heightened engagement and visual processing.
- Source localization suggested increased activation and functional connectivity in brain areas related to visual processing and spatial orientation during *Upsight*.
- *Upsight* resembles normal vision more than VMI, imagination, and visual hallucinations.

Human visual experiences do not solely rely on external light stimuli but extend to mental experiences where the mind constructs (or reconstructs) visual representations without direct external stimuli, such as visual mental imagery (VMI), imagination, or visual hallucinations (Palmer, 1999). Visual experiences are a cornerstone of human perception, offering a rich tapestry of sensations that shape our understanding of the world. This case study explores the unique perceptual phenomenon of *Upsight*, a visual experience reported by an individual following a mental health crisis at the end of 10 years of substance abuse and mental health challenges. Its phenomenology includes a continuous stream of vivid images that scroll holographically over his visual field, overlapping and persisting without the need to allocate attention to them (see Fig. 1). The holographic images are typically monochromatic with a single-color tint, most of the time purple. The individual reports occasional veridicality of the images and interprets the experience as being potentially the perception of another reality (e.g., non-physical or multiverse). Although the images do not directly correlate with concurrent thoughts, the individual can volitionally modify them upon closer attention, altering their form and content.

Figure 1

Artistic Illustration of the Upsight Phenomenon. A) Normal Vision. B) Upsight.

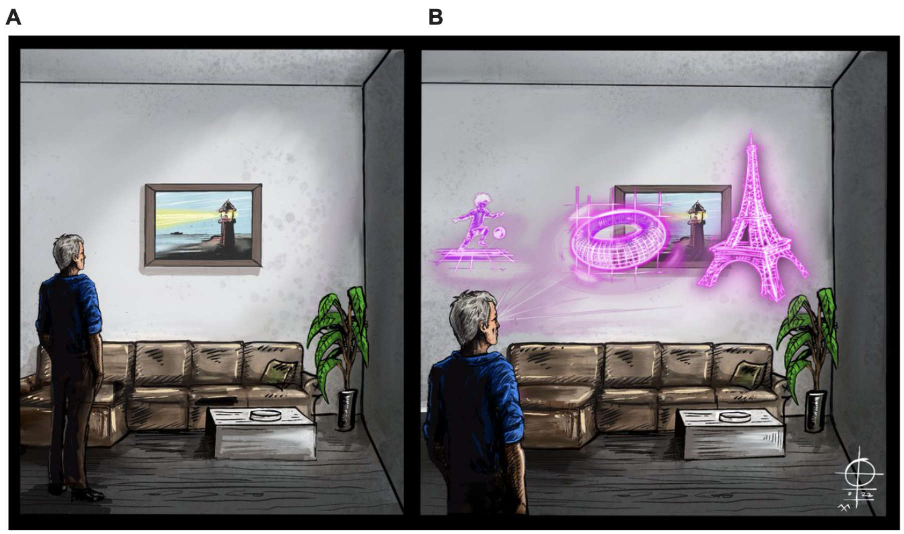

This case study aims to better understand this experience from a neuroscientific point of view using noninvasive electroencephalography (EEG). EEG offers several advantages over functional magnetic resonance imaging (fMRI) or positron emission tomography (PET) for investigating this type of phenomenon, including high temporal resolution, noninvasiveness, cost-effectiveness, portability, and comfort. Modern EEG source localization techniques enable estimation of the brain regions and networks involved, addressing the low spatial resolution problem.

We first review the most common human visual experiences (visual mental imagery, imagination, visual hallucinations) and their neural correlates. Then, we try to identify how *Upsight* experienced by a specific individual may relate to or differ from them based on the EEG activity at the scalp and source levels. We hypothesize that *Upsight* may involve similar processes to visual mental imagery (VMI).

Visual Perception

The visual cortex constructs images by processing electrical signals from the photoreceptors in the retina when they detect photons (light) from the environment. These signals travel via the optic nerve to the lateral geniculate nucleus (thalamus) and the primary visual cortex (V1), where basic features like edges and orientations are detected. The information is then transmitted to the secondary visual cortex (V2) to integrate more complex patterns (e.g., contours), followed by visual areas V3, V4, and V5 for processing form, color, and motion, respectively. Higher-level visual areas, such as the inferior temporal cortex and posterior parietal cortex, refine the information for object recognition, visual memory, and spatial awareness, culminating in a coherent visual perception (Bear et al., 2020).

At the scalp level, event-related potential (ERP) studies have identified several key components including P1 (the positive deflection occurring ~100 ms after stimulus onset over occipital and parietal regions; Luck, 2005) and N1 (a negative deflection peaking ~150-200 ms associated with selective attention prominent over the posterior scalp; Vogel & Luck, 2000). Later components, such as the P300 (peak ~300 ms), are linked to higher-order cognitive processes including stimulus evaluation and decision-making (Polich, 2007).

EEG functional connectivity studies have revealed that visual perception involves dynamic interactions between occipital, parietal, and frontal regions. These interactions are particularly evident in the beta (13-30 Hz) and gamma (30-100 Hz) frequency bands, associated with higher-order cognitive functions and sensory processing, respectively (Varela et al., 2001). fMRI studies further corroborate these findings by demonstrating that visual perception is supported by a distributed network that includes V1, lateral occipital cortex, and regions of the dorsal and ventral streams. These areas show increased connectivity during tasks requiring visual attention and object recognition (Friston, 2011).

Visual Mental Imagery (VMI)

VMI is the ability to mentally generate and manipulate visual images in the absence of external visual stimuli, typically based on memory and past visual experiences. VMI exhibits large interindividual differences, ranging from aphantasia, where individuals cannot voluntarily visualize mental images (Hart & Hay, 2022), to hyperphantasia, characterized by an enhanced ability to create vivid and very detailed mental images (Zeman et al., 2016, 2020). Participants with aphantasia report an elevated rate of difficulty with face recognition and autobiographical memory, not linked to deficits in intelligence or creativity. It does not seem to be because of a lack of metacognitive awareness of VMI and is different from visual agnosia (inability to recognize and identify objects or faces despite having normal vision). On the other hand, people with hyperphantasia report an elevated rate of synesthesia.

Early visual areas (e.g., V1, V2) were previously thought to play a key role in VMI, similar to visual perception but without inputs (Kosslyn et al., 2001; Pearson et al., 2015).

Journal of Anomalous Experience and Cognition (JAEX) 2025, Vol. 5, No. 2, pp. 136-167

However, recent studies showed that VMI mainly relies on the left-lateralized temporal network with the "fusiform imagery node" at its core (i.e., the left fusiform gyrus, a high level visual area; Spagna et al., 2021), with additional involvement of the posterior cingulate cortex (PCC) and the frontoparietal network (attentional and executive control network). Patients with brain damage in the occipital cortex retain vivid VMI. In contrast, damage extending into the temporal lobe, particularly in the left hemisphere, results in VMI impairments. Hence, VMI does not significantly engage early visual cortices but relies on higher-order associative areas, particularly in the left temporal lobe.

VMI has been extensively studied using electroencephalography (EEG). At the scalp level, changes in alpha band (8-13 Hz) activity, particularly alpha desynchronization over occipital and parietal regions, have been associated with visual imagery tasks (Kosslyn et al., 1995). This decrease in alpha power reflects increased cortical activation in areas involved in visual processing. Increased beta band (13-30 Hz) activity in visual areas has also been linked to VMI, indicating active engagement of these regions (Jensen et al., 2010). ERPs such as the N170 and P300 components have been observed to be modulated by visual imagery tasks (Morgan et al., 2008).

Source localization studies have revealed activation of the occipital and parietal cortex, regions known for their roles in visual processing and spatial attention during VMI (Kosslyn et al., 2001). Furthermore, the frontal cortex, particularly the prefrontal and dorsolateral prefrontal areas, has been implicated in the control and manipulation of mental images (Kosslyn et al., 2001). Activation in the temporal cortex has also been reported, particularly in tasks involving complex object or scene imagery (Ganis et al., 2004). These findings suggest that visual mental imagery engages a network of brain regions similar to those involved in visual perception, highlighting the intricate neural mechanisms underlying this cognitive process.

Visual Imagination

Visual imagination diverges from VMI by generating novel, often fantastical or abstract images that may not be rooted in past experiences, leading to unique visual constructs beyond ordinary objects. While engaging similar neural processes and regions as VMI, visual imagination also recruits networks associated with creativity and abstract thinking, such as the Default Mode Network (DMN) and executive control network, involving additional regions such as the medial prefrontal cortex and the anterior cingulate cortex (ACC; Beaty et al., 2016; Ishai et al., 2002). These networks are crucial for generating new content and integrating diverse ideas. Increased functional connectivity (FC) between the prefrontal cortex and other brain areas is associated with the integration and creation of new visual constructs. Research has shown increased FC between the DMN and executive control network, during creative idea production (Beaty et al., 2015). These findings highlight the complex interplay of neural networks in supporting the creative and generative aspects of visual imagination. This cooperation highlights how brain networks interact to support complex cognitive processes, especially goal-directed, self-generated thought.

Visual Hallucinations

Unlike VMI and imagination, which are under conscious control and internally driven, visual hallucinations are involuntary and often perceived as real and can arise involuntarily in the context of psychiatric disorders and neurological conditions, or voluntarily when induced through substance use. The phenomenology of visual hallucinations can range from simple flashes or geometric shapes to intricate and vivid scenes or figures. Neuroimaging studies suggest that they often involve hyperactivity in visual processing areas as well as disruptions in the connectivity between these regions and other parts of the brain (Collerton et al., 2005; Shine et al., 2015).

Key areas implicated in visual hallucinations include the visual cortex, thalamus, temporal lobe, and limbic system. Aberrant activity in the primary and secondary visual cortices can lead to the generation of hallucinatory images. The thalamus, which relays sensory information, may also play a role by improperly filtering visual signals. The temporal lobe (particularly the inferior temporal cortex), is involved in object recognition and can contribute to hallucinations when its activity is disrupted. The limbic system, including the amygdala and hippocampus, can influence the emotional content and vividness of hallucinations through its connections with the visual processing areas (Shine et al., 2015). Enhanced FC between these regions can further exacerbate hallucinatory experiences, whereas disrupted FC between the temporal lobe and other sensory processing areas can lead to the misinterpretation of visual information (Collerton et al., 2005). Alterations in neurochemical balances, such as in dopamine and serotonin, have also been implicated in the generation of visual hallucinations. Unlike the constructive nature of imagination and imagery, hallucinations are typically disruptive and often lack the individual's control or creative input (Collerton et al., 2005; Shine et al., 2015).

Charles Bonnet Syndrome (CBS) is characterized by highly detailed and complex visual hallucinations in individuals with significant vision loss, such as from age-related macular degeneration, glaucoma, or cataracts. These hallucinations can include intricate patterns, people, animals, or vivid scenes. Unlike other types of hallucinations, individuals with CBS typically retain insight and understand that these visual experiences are not real, distinguishing them from psychiatric conditions where insight may be impaired. The brain compensates for the lack of visual input by generating these images, leading to the vivid and detailed nature of the hallucinations (Menon et al., 2003; Teunisse et al., 1996).

How Does *Upsight* Relate to and Differ from These Visual Experiences?

VMI involves the mental visualization of objects, scenes, or events that are not currently being perceived. Like VMI, *Upsight* allows the individual to volitionally modify the images, suggesting a degree of conscious control over the experience. However, unlike typical VMI, which is internally driven and often correlates with concurrent thoughts (Kosslyn et al., 2001), the images in *Upsight* persist regardless of focused attention and do not directly correlate with the individual's current thoughts. This continuous and overlapping nature of the images in *Upsight* distinguishes it from the more transient and thought-linked visual imagery.

Upsight shares some characteristics with visual imagination in that the individual can alter the form and content of the images upon closer attention, indicating an element of creativity and generativity (Beaty et al., 2015). However, unlike imagination, which is typically an active and intentional process, *Upsight* appears to be a passive and continuous stream of images that occurs involuntarily, only becoming modifiable when the individual focuses on them. This involuntary aspect sets *Upsight* apart from the more deliberate and controlled nature of visual imagination.

Like hallucinations, the images in *Upsight* have a sense of reality and occasional veridicality, meaning they can sometimes be perceived as real. Visual hallucinations can also be continuous and holographic, superimposing onto the visual field, as seen in conditions like Charles Bonnet Syndrome (CBS), where individuals with visual impairments experience vivid and detailed hallucinations (Teunisse et al., 1996). However, a key difference is that the individual with *Upsight* retains the ability to modify the images voluntarily, a level of control typically absent in visual hallucinations. Furthermore, CBS is generally associated with significant vision loss and corresponding brain changes in the visual system (Teunisse et al., 1996), whereas *Upsight* does not necessarily imply such extensive visual impairment. In sum, although *Upsight* shares certain features with visual imagery, imagination, and hallucinations, it also presents unique characteristics that distinguish it from them.

Journal of Anomalous Experience and Cognition (JAEX) 2025, Vol. 5, No. 2, pp. 136-167

Study Aims

This study aimed to better understand the visual experience of *Upsight* by comparing it to visual mental imagery (VMI). The study involved presenting images that the participant then either visualized via VMI or via *Upsight* for 30 s following the presentation (with eyes closed in both cases). EEG, combined with source localization techniques, was used to assess which brain regions and networks differed the two conditions. This comparison helped determine whether *Upsight* shares more characteristics with VMI (e.g., hyperphantasia) or if it aligns more closely with imagination or visual hallucinations.

Hypotheses

1. Given the ability to volitionally modify the images, we hypothesized that the neural activity during *Upsight* would share significant overlap with visual mental imagery, involving particularly the left temporal region involved in VMI.
2. Unlike traditional hallucinations, we hypothesized that *Upsight* would show unique neural connectivity patterns, possibly involving enhanced connectivity in networks related to attention and sensory integration, reflecting its continuous and modifiable nature.

Method

Participant

The participant was a 59-year-old Caucasian male who reported developing the new experience after a severe mental health crisis. At that time, he met the criteria for substance dependence as well as substance-induced psychotic disorders, which involved the use of cocaine and methamphetamines with paranoia, hallucinations, delusions, and characteristics of mania such as grandiosity and compulsive shopping/spending. His mental health crisis ended in 2012. His last use of cocaine was in December of 2012, also the first time he saw these *Upsight* images. The images have been consistently vivid and detailed from the beginning. He reports no use of alcohol or other mind-altering substances since 2012 and has good current psychosocial functioning. He does report mild symptoms of post-traumatic stress from his previous substance use episodes, such as proneness to sensory overload and higher sensitivity

2025, Vol. 5, No. 2, pp. 136-167

Journal of Anomalous Experience and Cognition (JAEX)

and vigilance. The participant is not currently on any medication or supplement and is not distressed by his new ability to see images, which do not interfere with his daily life or normal perception. Two fMRIs (in 2012 and 2015) showed no brain damage or abnormalities, ruling out CBS which typically involves lesions in visual regions. Neurologists speculate that drugs may have rewired his brain or opened a new neural pathway, but there were no definitive clinical answers. The term *Upsight* was coined by his wife, as he typically looks up when focusing on the images. He has been in contact with a few others who have reported a similar experience. The participant approached the research team with an interest in better understanding this phenomenon. All study activities were approved and overseen by the Institutional Review Board at the Institute of Noetic Sciences (IORG#0003743). The participant provided written informed consent to participate in this study and volunteered his time.

Design

Randomly selected images were presented to the participant while seated in a chair in front of a computer screen in a dimly lit room. Four experimental sessions were completed over two days (two per day with a 15-minute break), enabling the collection of data from a total of 200 trials per condition across all runs and sessions (50 per condition for each run, for a total of 400 trials). Visual stimuli from the International Affective Picture System (IAPS; Lang et al., 2008) were controlled by a program written for the study using the MATLAB Psychophysics Toolbox (Brainard, 1997). The IAPS dataset was used because it provides a large set of standardized, high-quality color photographs suitable for controlled experimental design. However, since the primary aim of this study was not to investigate emotional processing, all images were prescreened to exclude those with high emotional valence or arousal—specifically erotic, aversive, or gruesome content. Each trial included the presentation of the same image twice, once for each condition. At the beginning of each trial, the audio prompt “Look at the image” instructed the participant to look at the image for 10 s. Then, the screen went blank and he was instructed to close his eyes for 30 s, and an audio recorded prompted him to either (a) visualize mentally the presented image (VMI), or (b) modulate the *Upsight* images such that the key element of the image was manifest for him to focus on. The audio prompts were, “Now recall the image” and “Now do *Upsight*,” respectively. At the end of the 30-s eyes-closed period, the audio prompt “Look at the image” instructed him to open his eyes and look at the same image a 2nd time for 10 s to perform the other condition on the same stimulus. The order of the two conditions was alternated randomly to control for potential habituation or other undesired order effects. The entire image presentation epoch lasted for 1 minute and 20 seconds (see Fig. 2). Immediately following the completion of each epoch, the next epoch began with a unique image (selected randomly from a pool of 200 images). The participant completed a practice session before starting the actual experiment to ensure that he was familiar with the task and stimuli. These practice images were not used in the subsequent task and practice trial data were not used in the analyses.

Figure 2

Study Design

Image	Recall Image*	Repeat Image	Upsight of Image*
10 seconds; eyes open	30 seconds; eyes closed	10 seconds; eyes open	30 seconds; eyes closed

EEG Data Collection

A 64-channel EEG was recorded at 1024 Hz with an ActiveTwo Biosemi system (Biosemi, Amsterdam, Netherlands). Electrodes were placed according to the 10-20 nomenclature (standard 64-channel EasyCap). SignaGel electroconductive gel was applied to each electrode and electrode impedance was kept below manufacturer guidelines (±20 kOhms). Event markers were sent to the EEG amplifier digital input channel using the Biosemi USB interface and saved along with the EEG data, synchronized with millisecond accuracy. One set of markers represented the onset of the image with its image identifier number and another set of triggers marked the condition. Event latencies, markers, and image identifiers were also saved in a separate text file as a backup.

EEG Data Processing

Electroencephalography (EEG) data were preprocessed in EEGLAB (Delorme & Makeig, 2004) with downsampling, bandpass filtering (0.5–45.5 Hz), reference electrode standardization technique (REST) re-referencing, abnormal channel removal with interpolation, and trial outlier rejection based on root mean square (RMS) amplitude and signal-to-noise ratio (SNR). Blind source separation used preconditioned independent component analysis for real data (PICARD; Ablin et al., 2018), and artifacts were removed via the independent component label (ICLabel) classifier (Pion-Tonachini et al., 2019). Source analysis, addressing volume conduction for more precise localization, was performed with the region-of-interest connectivity (ROIconnect) plugin (Pellegrini et al., 2023) using linearly constrained minimum variance (LCMV) beamforming and the Colin24 atlas (68 regions). Power spectral density (PSD) was computed via the Welch method, and functional connectivity (FC) was estimated using the multivariate interaction measure (MIM) on source-reconstructed data at the peak frequency of scalp and source power effects. See Supplementary Data for full details.

Single-Trials Statistics (Within-Participant)

A mass-univariate, non-parametric approach was used for statistical analysis (Maris & Oostenveld, 2007), using a 1,000-iteration bootstrap to estimate the null hypothesis (H0, the absence of a difference between the two conditions). Pairwise comparisons between the two conditions were performed using Yuen *t* tests (20% trimmed means) to better control for naturally skewed distributions and outliers (Yuen, 1974). The mass-univariate approach for EEG data involves performing statistical tests on each electrode or time point separately to determine the significance. This statistical approach is robust in handling complex datasets and can provide comprehensive insights into neural dynamics (Maris & Oostenveld, 2007), but this approach leads to a large number of comparisons (64 electrodes, 89 frequency bins) and, therefore, a higher chance for false positives (family-wise or type 1 errors). To address this problem, statistical outputs were corrected using spatiotemporal cluster correction, per guidelines (Mensen & Khatami, 2013; Pernet et al., 2015) at the 99.9% confidence level (i.e., $p < .001$).

The same algorithm was used for nonparametric statistics for the spectral power analysis at the brain area level. However, to perform spatiotemporal cluster correction on the source data, we had to obtain a neighbor matrix of the brain areas, which contain many voxels in 3D space. We took the Cartesian center of each brain area and then used the same algorithm as for scalp EEG electrodes to estimate the brain area neighbors. In brief, the 3D center coordinates are projected onto a 2D plane via polar projection. Delaunay triangulation is then performed on these 2D projected points, and the neighbor matrix is constructed by identifying area pairs that share edges in the Delaunay triangulation. Neighbors that were too far away (3 standard deviations from the mean) were removed.

For spectral power analyses (scalp and source), the main plot displays the mass-univariate differences after correction across all electrodes or brain areas (y-axis) and frequencies (x-axis). Details about the significant clusters are reported in the text. The frequency with the highest *t* value was further examined using a scalp topography (for scalp data) and a cortex surface projection (for source data) to inform on the distribution and location of the effects. For the scalp topography, significant EEG channels are displayed as black dots. Similarly, the EEG channel or brain area with the highest *t* value was further examined using the PSD distribution for each condition. The main curves correspond to the 20% trimmed means (across trials) and the shaded areas show the 95% quantile intervals computed with a 1,000-iterations Bayesian bootstrap (better suited for skewed distributions and providing more intuitive interpretations than Frequentists confidence intervals or high-density intervals; Etz et al., 2024), for good practice. Black horizontal bars on the x-axis (if any) indicate significant differences after spatiotemporal cluster correction.

For functional connectivity (FC), we only took the values for frequency of interest (i.e. 11 Hz where the main effect was observed in spectral power analysis) and used the EEGLAB *statcondfieldtrip* function to perform bootstrap statistics ($p < .001$; 1,000 iterations; spatiotemporal cluster correction for type 1 error). For visualization we provide the masked connectivity matrix (showing only the significant effect after correction for multiple comparisons), and the same surface cortex projection as for the source spectral power analysis.

Results

Scalp Analysis - Spectral Power

Analyses of the EEG data at the scalp level indicate significant widespread differences ($p < .001$ after spatiotemporal cluster correction for type 1 error) between the *Upsight* and the visual mental imagery (VMI) conditions (Fig. 3A). Six main significant clusters were observed:

Cluster 1: 1.5-2.5 Hz, with peak effect at channel O2 at 1.5 Hz (t = -6.8; df = 110)

Cluster 2: 4-26 Hz, with peak effect at channel PO8 at 11 Hz (t = -19.5; df = 110).

Cluster 3: 28.5-32.5 Hz, with peak effect at channel F8 at 31 Hz (t = 8; df = 110)

Cluster 4: 39.5-41 Hz, with peak effect at channel F8 at 40 Hz (t = 7.2; df = 110)

Cluster 5: 42.5-45 Hz, with peak effect at channel F8 at 45 Hz (t = 7.6; df = 110)

Cluster 6: 39-45 Hz, with peak effect at channel O1 at 40 Hz (t = 6.5; df = 110)

Note that the clusters are computed in 3-D scalp space x space x frequencies, so it is not possible to represent them on the 2-D channels x frequency representation of Fig. 3A. Additionally, a smaller positive cluster was observed around 8–9 Hz at frontal electrodes, though its effect size was modest compared to the primary clusters and is not further discussed.

In sum, we observed large spectral power decreases in low frequencies (1-26 Hz) and increases in higher frequencies (28-32 Hz and 39-45 Hz), during *Upsight* relative to VMI. The largest effect was observed at 11 Hz widespread in the posterior electrode sites but was widespread across all electrode sites, displaying significantly less alpha power during the *Upsight* condition relative to the VMI condition (Fig. 3B and 3C). The power spectral density (PSD) distribution at EEG channel PO8 is visible in Fig. 3B, depicted by the 20% trimmed mean of each condition and the 95% quantile intervals (shaded areas). And the scalp topography in Fig. 3C displays the distribution of the corrected effects at 11 Hz on the scalp surface.

2025, Vol. 5, No. 2, pp. 136-167

Journal of Anomalous Experience and Cognition (JAEX)

Source Analysis - Spectral Power

At the brain area level (after source localization and source reconstruction), we also observed a strong significant difference in the alpha band ($p < .001$ after spatiotemporal cluster correction for multiple comparisons) between *Upsight* and the control conditions (i.e., image recall). One main cluster was observed from 1 to 27.5 Hz, with a peak effect in the parietal lobule right at 11 Hz (t = -18; df = 110; Fig. 1A). The power spectral density distribution at the superior parietal lobule right is visible in Fig. 4B, depicted by the 20% trimmed mean of each condition and the 95% quantile intervals (shaded areas). Additionally, the cluster difference at 11 Hz is also projected onto a cortex surface for better visualization of the corrected effect (Fig. 4C), showing that the decrease is mainly located in the occipital, parietal, and temporal regions. Note that the decrease is slightly superior in the right hemisphere for the temporoparietal areas. A second, smaller cluster was observed from 33-45 Hz, with a peak decrease in the isthmus cingulate left at 36 Hz (t = -7.1; df = 110). More details on which brain areas showed the strongest differences and corresponding interpretations can be found in the discussion.

Figure 3

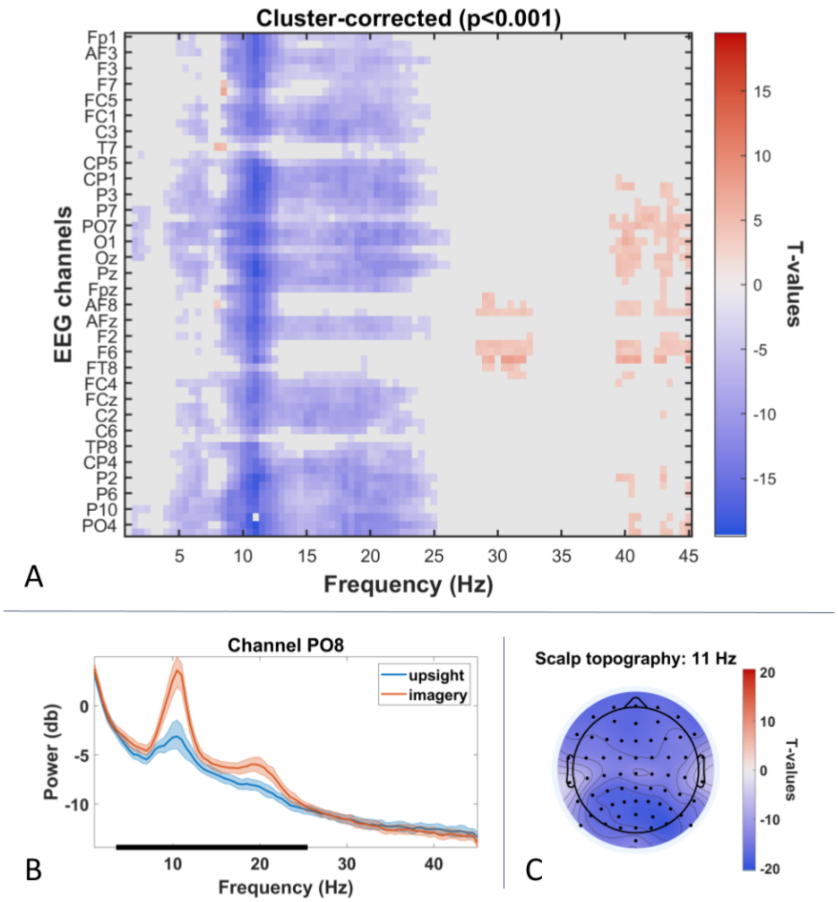

Note: **A**.Mass-univariate analysis at the scalp level (electrodes) showing widespread decrease in spectral power in frequencies 5-25 Hz (blue) during ***Upsight*** relative to visual mental imagery (VMI). **B.** Power spectrum of each condition at the electrode with the strongest difference (i.e., PO8), with a black horizontal bar indicating the statistically significant difference (Peak at 11 Hz; t = -19.5). The lines represent the 20% trimmed mean across trials, and shaded areas the 95% quantile intervals. **C.** Scalp topography at the frequency with the strongest difference (i.e., 11 Hz).

Figure 4

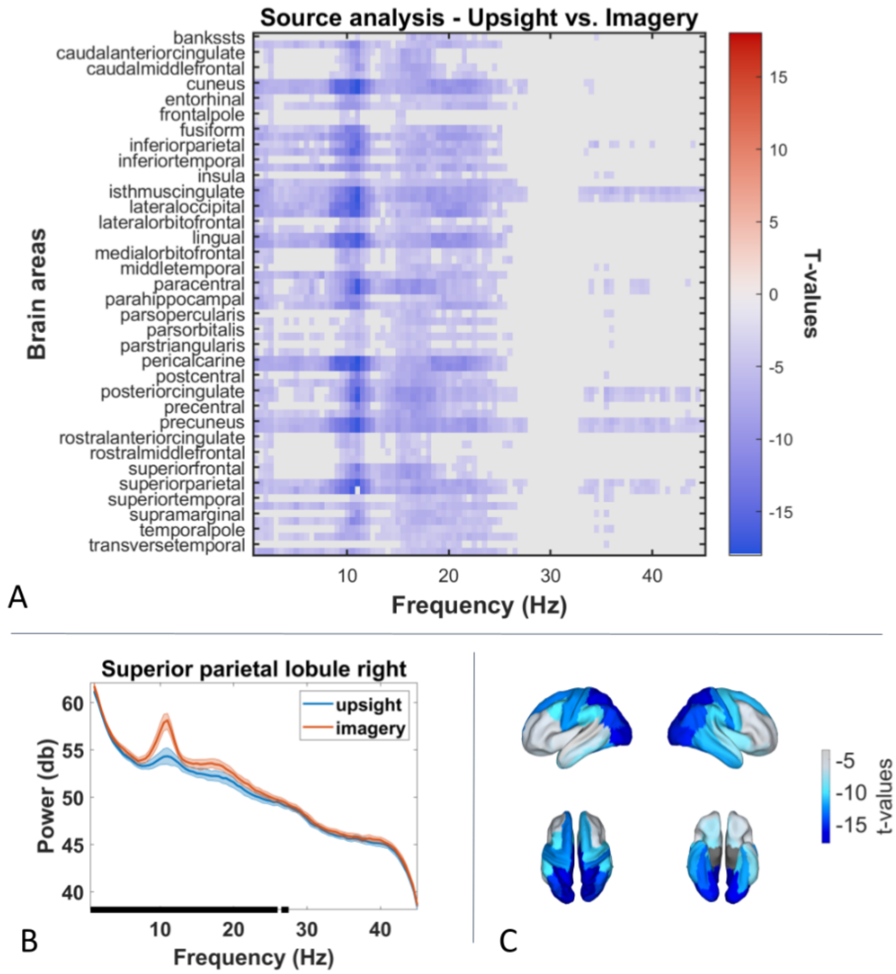

Note: **A.** Mass-univariate analysis at the source level (brain areas averaged across both hemispheres) showing widespread decrease in spectral power in frequencies 1-27 and 33-45 Hz (in blue) during ***Upsight*** relative to visual mental imagery (VMI). **B.** Power spectrum of each condition at the brain area with the strongest difference (i.e., superior parietal lobule right), with a black horizontal bar indicating the frequencies with statistically significant differences (Peak at 11 Hz; t = -18). The lines represent the 20% trimmed mean across trials, and shaded areas the 95% quantile intervals. **C.** Cortex surface projection at the frequency with the strongest difference (i.e., 11 Hz).

Source Analysis – Functional Connectivity

The functional connectivity (FC) analysis ($p < .001$ and spatiotemporal cluster correction for type 1 error) revealed significant pairs of brain regions with decreased alpha power (11 Hz) during the *Upsight* condition relative to visual mental imagery (VMI). Area pairs that showed the strongest differences are the left inferior and superior parietal lobe (t = -11.19), posterior cingulate (left) with the cuneus left (t = -10.79)

Journal of Anomalous Experience and Cognition (JAEX) 2025, Vol. 5, No. 2, pp. 136-167

and right (t = -10.53), postcentral gyrus (left) with the cuneus (left) (t = -10.45) and pericalcarine (left) (t = -10.31), and pericalcarine cortex (left) with the paracentral lobule (left; t = -10.28). Additional significant pairs include the posterior cingulate (right) with the cuneus (right) (t = -10.26), superior parietal lobe (left) with posterior cingulate (left; t = -10.14), supramarginal gyrus (left) with superior parietal lobe (left) (t = -10.05) and cuneus (left) (t = -9.87), and posterior cingulate (left) with the pericalcarine cortex (left) (t = -10.45). Note that there is no directionality to this measure.

Key pairs include the posterior cingulate (right) with the cuneus (right; $t = -10.26$), the posterior cingulate (left) with the inferior parietal lobe (left; $t = -9.81$), and the precuneus (left) with the caudal anterior cingulate (left; $t = -9.85$) (Leech & Sharp, 2014). These connections indicate a robust network supporting the integration of visual-spatial memory and self-referential thought. Additionally, the superior parietal lobe (left) connecting with the posterior cingulate (left; $t = -10.14$) suggests coordinated processing of spatial and memory-related information.

These findings support our initial hypotheses. First, the overlap in neural activity between *Upsight* and VMI—particularly the modulation of alpha power and engagement of visual and cognitive networks—supports Hypothesis 1, suggesting that *Upsight* shares neural mechanisms with VMI. Second, the distinct spatial patterns of alpha power reduction and functional connectivity, especially the involvement of sensory integration and attention-related regions, support Hypothesis 2 by highlighting that *Upsight* is neurophysiologically distinct from traditional or CBS-type hallucinations.

Discussion

This study examined the neural mechanisms underlying the visual phenomenon known as “Upsight,” in which an individual perceives continuous, detailed holographic images overlaid on his visual field. Results showed that Upsight is associated with a significant decrease in alpha and delta power across the scalp, particularly in posterior regions, and an increase in gamma power (29-45 Hz) in right frontal and left posterior areas. These findings suggest heightened cortical activation, particularly in cognitive and visual processing networks. Source-level analysis further revealed decreased alpha power and functional connectivity in brain areas responsible for visual perception, spatial orientation, and sensory integration, indicating increased activity and engagement of these regions.

Figure 5

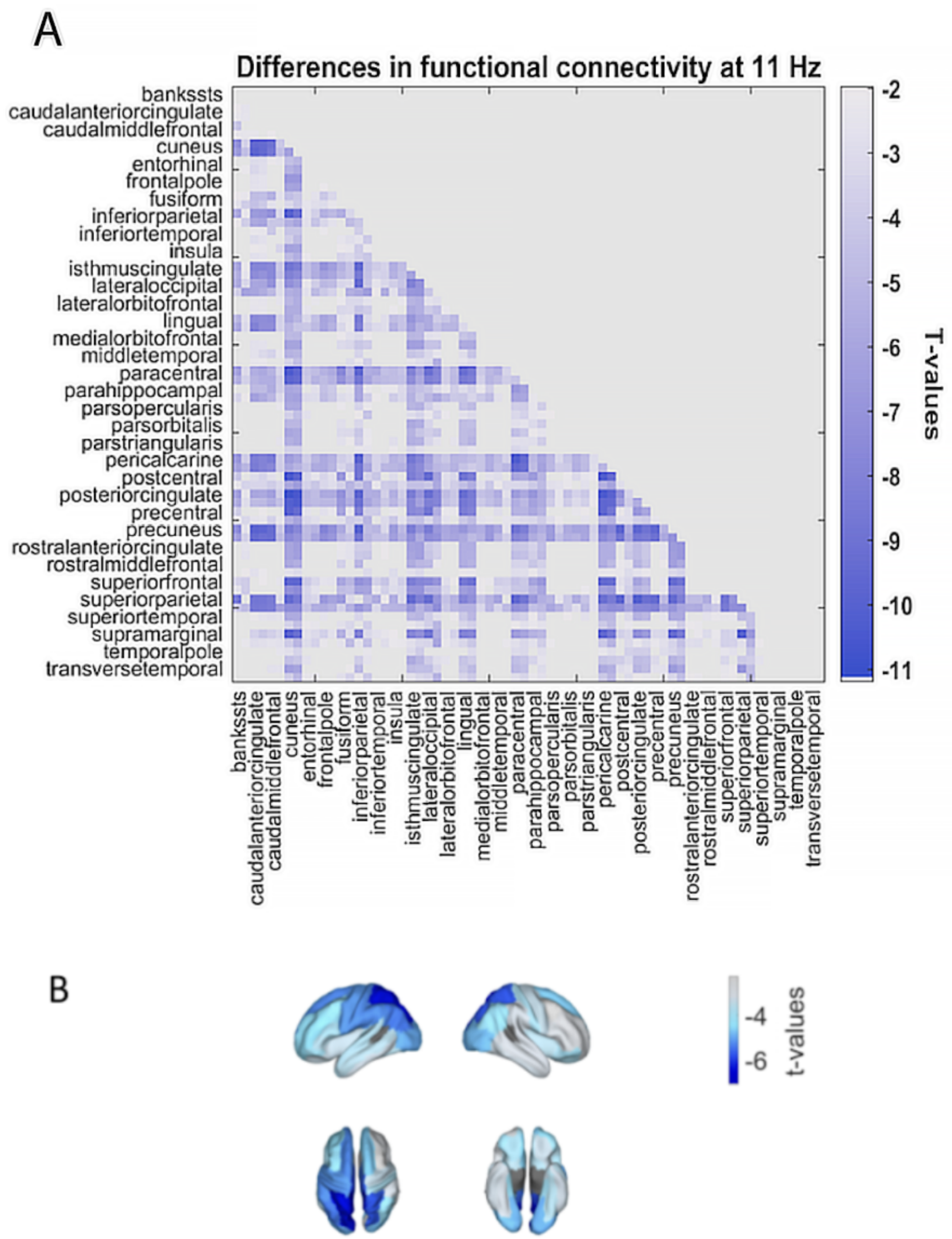

Note: **A**. Functional connectivity matrix of the differences ***Upsight*** vs visual mental imagery (VMI), at 11 Hz (peak of the effect at the scalp and source levels). Each brain area is represented by two rows/columns, where the first corresponds to the left cortex and the second to the right cortex. **B.** Cortex surface projection of the same results to ease interpretation.

Scalp Power

We noted a strongly significant reduction in alpha power (8-13 Hz) during *Upsight* compared to the control condition. This decrease was widespread across all scalp electrodes at 11 Hz, indicating a global decrease in the alpha frequencies and, to a smaller extent, in the beta frequencies (15-25 Hz). Functionally, alpha oscillations play a key role in attentional control and gating of perceptual awareness (Hanslmayr et al., 2011; Mazaheri et al., 2014). They are typically noticeable in posterior visual areas when the eyes are closed (so-called alpha synchronization or resting state alpha) or in idle states with reduced cognitive effort (e.g., relaxed wakeful state). Alpha oscillations are typically associated with inhibiting local cortical regions (Jensen & Mazaheri, 2010; Klimesch et al., 2007; Mathewson et al., 2011). Thus, the strong, widespread decrease in alpha power during the *Upsight* condition relative to VMI suggests a large reduction in cortical inhibition and, therefore greater cortical activation during *Upsight,* with the strongest manifestation in the posterior scalp regions.

Additionally, the scalp analysis revealed increased activity during *Upsight* relative to VMI in the higher-frequency range, the 28.5-32.5 Hz range, particularly in the frontal regions, and the 39-45 Hz range, with significant effects in both the frontal and occipital regions (see scalp topographies in Supplementary data). The increased high-frequency activity in the frontal regions highlights the participant's heightened engagement in executive and cognitive control processes during *Upsight* (Engel & Fries, 2010; Fries, 2009). Meanwhile, the increased activity in the occipital regions suggests enhanced visual processing and integration of the continuous *Upsight* visual inputs.

Finally, we observed a significant decrease in the delta band during *Upsight* relative to VMI in the posterior regions. Although increased delta power (1-3 Hz) is often associated with deep sleep or ocular artifacts (in frontal regions), it is also linked to "cortical deafferentation," or the inhibition of sensory inputs that interfere with internal concentration during cognitive tasks (Harmony, 2013).

Source Power

The brain areas with the strongest decrease in alpha power were: 1) the superior parietal lobule (right) involved in spatial orientation and attention, suggesting heightened engagement in spatial processing and sensory integration during *Upsight* compared to VMI (Wolpert et al., 1998). 2) The pericalcarine cortex (left and right), part of the primary visual cortex (V1) responsible for initial visual processing, implying increased visual processing activity due to the vivid and continuous nature of the holographic images (Wandell et al., 2007). 3) The cuneus (left and right), associated with basic visual processing, attention, and memory, indicating enhanced visual processing and attention during *Upsight* (Vanni et al., 2001). 4) The isthmus cingulate (left), which integrates visual-spatial memory and emotional regulation, reflecting enhanced emotional and cognitive integration during *Upsight*, potentially contributing to the sense of reality and importance of the images (Leech & Sharp, 2014). 5) The fusiform gyrus (left and right), crucial for object recognition and face processing, indicates heightened activity in processing detailed visual content (Kanwisher et al., 1997). 6) The inferior parietal lobule (left), which plays a role in spatial attention and perception, suggests increased demand for attention and integration of spatial information (Husain & Nachev, 2007). 7) The supramarginal gyrus (left), involved in spatial awareness and perception, suggests enhanced engagement in processing spatial aspects of the visual field (Silani et al., 2013). 8) The middle temporal gyrus (left and right), associated with processing visual motion and object recognition, indicates heightened activity in interpreting dynamic and complex visual images (Allison et al., 1999).

Note that we observed that the significant high-frequency power increase in the occipital and frontal regions seen in sensor-level data disappears, likely due to a poor signal-to-noise ratio. Since source analysis may amplify some noise, less significant results in the channel space tend to vanish.

Source Functional Connectivity

The functional connectivity (FC) analysis revealed significant decreases in alpha-band (11 Hz) connectivity during the *Upsight* condition compared to visual mental imagery (VMI), primarily involving the cuneus, pericalcarine cortex, posterior cingulate cortex, superior and inferior parietal lobules, and supramarginal gyrus. These reductions in connectivity were widespread across regions associated with visual processing, spatial orientation, and sensory integration (e.g., cuneus, pericalcarine cortex), as well as areas implicated in attention and memory (e.g., posterior cingulate, parietal lobes).

These findings suggest a reorganization of functional interactions within the visual and attentional networks during *Upsight*. Specifically, the observed connectivity decreases among posterior cortical regions may reflect a shift toward more localized or differentiated processing, in contrast to the integrative network coordination typically seen during VMI. The visual processing network—comprising early visual cortices

Journal of Anomalous Experience and Cognition (JAEX) 2025, Vol. 5, No. 2, pp. 136-167

(e.g., pericalcarine, cuneus), parietal regions, and the posterior cingulate—is known to support the integration of perceptual and mnemonic information during internally generated visual tasks (Leech & Sharp, 2014; Vanni et al., 2001; Wandell et al., 2007).

Importantly, these connectivity changes parallel the strong decreases in alpha power observed in the same regions, suggesting a unified mechanism of reduced inhibition and heightened local activation. This concurrent reduction in both alpha power and inter-regional alpha-band synchronization indicates that *Upsight* engages a more autonomous and possibly more sensory-driven mode of visual processing than VMI, relying less on the coordinated top-down modulation characteristic of imagery and more on sustained bottom-up or intrinsic sensory activity.

Overall, scalp results revealed that *Upsight* is characterized by decreased alpha and delta power, and increased gamma power, indicating a broad increased cortical activation. Analyses at the source level showed enhanced activity and connectivity between brain regions involved in visual processing, spatial orientation, and sensory integration, suggesting well-coordinated networks supporting the vivid and continuous visual experiences of *Upsight*.

Imagination, which engages creative and generative processes involving the medial prefrontal cortex and other higher-order cognitive areas, differs from *Upsight* as it is typically an active and intentional process. In contrast, *Upsight* appears to be more passive and continuous, lacking the deliberate and creative input seen in imagination.

Similar to visual hallucinations in conditions like schizophrenia or Charles Bonnet Syndrome (CBS), we observed increased activity and FC in visual processing areas, compared to VMI. However, unlike the often fragmented and less detailed hallucinations seen in schizophrenia, *Upsight* involves continuous and highly detailed visual experiences. This pattern bears some resemblance to CBS, but the participant does not have the typical visual impairments in visual regions and resulting hyperactivity of visual areas that lead to the visual hallucinations. Also, CBS typically involves uncontrollable visual hallucinations, whereas *Upsight* appears to involve more structured and continuous visual experiences that can be modulated to some extent, indicating an organized involvement of executive and attention networks. On the other hand, complex visual hallucinations reflect dysfunction within and between these networks, leading to inappropriate interpretation of ambiguous percepts (Shine et al., 2015). These distinctions highlight the unique neural mechanisms underpinning *Upsight*, setting it apart from other visual experiences such as VMI, imagination, and hallucinations.

The participant reported experiencing *Upsight* during the VMI task and needing to block it out to focus, consistent with our findings of increased delta and alpha power, indicating greater inhibitory effort. In contrast, *Upsight* itself showed higher engagement with visual holographic inputs, reflected by elevated power in higher frequencies and reduced delta and alpha power. These observations suggest that the participant's increased alpha activity during VMI may signify active inhibition of holographic images, supporting the alpha inhibition hypothesis, while decreased inhibition during *Upsight* aligns with heightened visual processing and engagement.

In sum, the present results provide empirical support for our hypotheses. The engagement of regions associated with VMI, including the fusiform gyrus and left-lateralized visual areas, aligns with Hypothesis 1, indicating that *Upsight* shares core features of internally generated imagery. However, the continuous, externally overlaid, and modifiable nature of *Upsight*, alongside distinct patterns of functional connectivity and reduced alpha synchrony in posterior regions, points to a broader cortical network engagement consistent with Hypothesis 2. This pattern is not characteristic of spontaneous hallucinations, thus distinguishing *Upsight* as a unique phenomenon.

To gain deeper insights into the phenomenon, a comprehensive psychological or psychiatric assessment would be beneficial to better characterize the context in which it occurs. Although such an assessment was beyond t this paper, incorporating it in the future could provide a more holistic understanding of the underlying factors and enhance the robustness of the findings.

We acknowledge the possibility of unconscious demand characteristics, given the participant's awareness of the conditions being tested. However, the alternating conditions design, with randomization sometimes resulting in two *Upsight* or two recall trials in a row, helps control for order or related expectation effects. Future studies could try to develop masking techniques to further minimize this potential effect.

In our study, we implemented 2 sessions on separate days and conducted 2 runs per day, with each run consisting of 50 trials per condition (2 conditions). We combined the EEG data from the different sessions, which can introduce several limitations, such as session-specific variability and adaptation effects (Luck, 2014). Additionally, EEG signals being inherently non-stationary, computing spectral power for each trial independently of the session can potentially introduce potential biases. However, considering the robust statistics employed and the strength of the effect observed, we consider these limitations as negligible. Furthermore, combining data from different sessions can also increase data robustness and control for temporal confounds such

Journal of Anomalous Experience and Cognition (JAEX) 2025, Vol. 5, No. 2, pp. 136–167

as time-of-day effects and fatigue. Future studies could implement a general linear model (GLM) analysis to mitigate these potential biases by incorporating sessions as a covariate (Monti, 2011).

We acknowledge that source reconstruction should always be interpreted cautiously. However, the methods employed in this study have been thoroughly validated by leaders in the field of EEG modeling and source reconstruction, ensuring high reliability and accuracy. Moreover, our results show strong coherence with the scalp-level findings, reinforcing the validity of our interpretations.

To further investigate the nature of the *Upsight* experience, it would be beneficial to compare it directly with visual perception. Future experiments could take the 10-s periods where the participant looked at the stimuli to create a 3rd condition of visual perception and compare that with the *Upsight* and VMI conditions. We did not wish to do this because these periods are eyes open and contain more ocular artifacts, but this approach could help determine whether *Upsight* more closely resembles visual perception regarding neural activation patterns, relative to VMI. Similarly, adding an imagination task could provide a more comprehensive understanding of how *Upsight* differs from the underlying neural processes. By including a task specifically designed to engage the imagination, we could further delineate the neural mechanisms unique to *Upsight*, VMI, and imagination, providing a clearer distinction between these states. However, designing such a task appropriately to approximate the *Upsight* and VMI conditions for comparison is challenging.

*Conclusion***.** In summary, our findings indicate that Upsight leads to a significant reduction in alpha and delta power across all brain regions, especially in posterior areas, alongside an increase in gamma power in right frontal and left posterior areas. Although this study advances our understanding of *Upsight*, future research should address these limitations and explore the proposed directions to provide a more comprehensive understanding of this unique visual experience. Notably, the homogeneity between source and scalp results suggests accurate solving of the inverse problem, reinforcing the validity of our findings. If more individuals report experiencing *Upsight* or similar phenomena, a group study could be conducted to provide more robust insights into this phenomenon.

Declaration: The authors declare no conflict of interest.

References

Ablin, P., Cardoso, J.-F., & Gramfort, A. (2018). Faster independent component analysis by preconditioning with Hessian approximations. *IEEE Transactions on Signal Processing*, *66*(15), 4040–4049. https://doi.org/10.1109/TSP.2018.2844203

Allison, T., Puce, A., Spencer, D. D., & McCarthy, G. (1999). Electrophysiological studies of human face perception. I: Potentials generated in occipitotemporal cortex by face and non-face stimuli. *Cerebral cortex*, *9*(5), 415-430.

Bear, M., Connors, B., & Paradiso, M. A. (2020). *Neuroscience*: *Exploring the brain, enhanced edition*: *Exploring the brain*. Jones & Bartlett Learning.

Beaty, R. E., Benedek, M., Kaufman, S. B., & Silvia, P. J. (2015). Default and executive network coupling supports creative idea production. *Scientific Reports*, *5*(1), 10964.

Beaty, R. E., Benedek, M., Silvia, P. J., & Schacter, D. L. (2016). Creative cognition and brain network dynamics. *Trends in Cognitive Sciences*, *20*(2), 87–95. https://doi.org/10.1016/j.tics.2015.10.004

Brainard, D. H. (1997). The psychophysics toolbox. *Spatial Vision*, *10*, 433–436.

Brisbon, N. M., & Lowery, G. A. (2009). Mindfulness and levels of stress: A comparison of beginner and advanced hatha yoga practitioners. *Journal of Religion and Health. 19949871*. https://doi.org/10.1007/s10943-009-9305-3

Briscoe, A. D., & Chittka, L. (2001). The evolution of color vision in insects. *Annual Review of Entomology*, *46*, 471–510. https://doi.org/10.1146/annurev.ento.46.1.471

Collerton, D., Perry, E., & McKeith, I. (2005). Why people see things that are not there: A novel perception and attention deficit model for recurrent complex visual hallucinations. *The Behavioral and Brain Sciences*, *28*(6), 737–757; discussion 757-794. https://doi.org/10.1017/S0140525X05000130

Delorme, A., & Makeig, S. (2004). EEGLAB: An open source toolbox for analysis of single-trial EEG dynamics. *Journal of Neuroscience Methods*, *134*, 9–21.

Engel, A. K., & Fries, P. (2010). Beta-band oscillations—Signalling the status quo? *Current Opinion in Neurobiology*, *20*(2), 156–165. https://doi.org/10.1016/j.conb.2010.02.015

Etz, A., Chávez de la Peña, A. F., Baroja, L., Medriano, K., & Vandekerckhove, J. (2024). The HDI and ROPE decision rule is logically incoherent but we can fix it. *Psychological Methods*. https://doi.org/10.1037/met0000660

Fries, P. (2009). Neuronal gamma-band synchronization as a fundamental process in cortical computation. *Annual Review of Neuroscience*, *32*(1), 209-224.

Friston, K. J. (2011). Functional and effective connectivity: A review. *Brain Connectivity*, *1*(1), 13–36.

Ganis, G., Thompson, W. L., & Kosslyn, S. M. (2004). Brain areas underlying visual mental imagery and visual perception: An fMRI study. *Cognitive Brain Research*, *20*(2), 226–241.

Hanslmayr, S., Gross, J., Klimesch, W., & Shapiro, K. L. (2011). The role of alpha oscillations in temporal attention. *Brain Research Reviews*, *67*(1), 331–343. https://doi.org/10.1016/j.brainresrev.2011.04.002

Harmony, T. (2013). The functional significance of delta oscillations in cognitive processing. *Frontiers in Integrative Neuroscience*, *7*. https://doi.org/10.3389/fnint.2013.00083

Hart, E., & Hay, L. (2022). Do you see what I see? Exploring vividness of visual mental imagery in product design ideation. *Proceedings of the Design Society*, *2*, 881–890.

Husain, M., & Nachev, P. (2007). Space and the parietal cortex. *Trends in Cognitive Sciences*, *11*(1), 30–36. https://doi.org/10.1016/j.tics.2006.10.011

Ishai, A., Haxby, J. V., & Ungerleider, L. G. (2002). Visual imagery of famous faces: Effects of memory and attention revealed by fMRI. *NeuroImage*, *17*(4), 1729–1741. https://doi.org/10.1006/nimg.2002.1330

Jensen, O., & Mazaheri, A. (2010). Shaping functional architecture by oscillatory alpha activity: Gating by inhibition. *Frontiers in Human Neuroscience*, *4*, 186. https://doi.org/10.3389/fnhum.2010.00186

Kaas, J. H. (1983). What, if anything, is SI? Organization of first somatosensory area of cortex. *Physiological Reviews*, 63(1), 206–231. https://doi.org/10.1152/physrev.1983.63.1.206

Kanwisher, N., McDermott, J., & Chun, M. M. (1997). The fusiform face area: A module in human extrastriate cortex specialized for face perception. *Journal of Neuroscience*, *17*(11), 4302–4311. https://doi.org/10.1523/JNEUROSCI.17-11-04302.1997

Kim, H., Luo, J., Chu, S., Cannard, C., Hoffmann, S., & Miyakoshi, M. (2023). ICA's bug: How ghost ICs emerge from effective rank deficiency caused by EEG electrode interpolation and incorrect re-referencing. *Frontiers in Signal Processing*, *3*. https://doi.org/10.3389/frsip.2023.1064138

Klimesch, W. (1999). EEG alpha and theta oscillations reflect cognitive and memory performance: A review and analysis. *Brain Research Reviews*, *29*(2–3), 169–195.

Klimesch, W., Sauseng, P., & Hanslmayr, S. (2007). EEG alpha oscillations: The inhibition–timing hypothesis. *Brain Research Reviews*, *53*(1), 63–88. https://doi.org/10.1016/j.brainresrev.2006.06.003

Kosslyn, S. M., Ganis, G., & Thompson, W. L. (2001). Neural foundations of imagery. *Nature Reviews Neuroscience*, *2*(9), 635–642.

Kosslyn, S. M., Thompson, W. L., Klm, I. J., & Alpert, N. M. (1995). Topographical representations of mental images in primary visual cortex. *Nature*, *378*(6556), 496–498.

Lang, P. J., Bradley, M. M., & Cuthbert, B. N. (2008). International Affective Picture System (IAPS): Affective ratings of pictures and instruction manual (Technical Report A-8). University of Florida, Gainesville, FL.

Leech, R., & Sharp, D. J. (2014). The role of the posterior cingulate cortex in cognition and disease. *Brain*, *137*(1), 12–32. https://doi.org/10.1093/brain/awt162

Luck, S. J. (2005). Ten simple rules for designing ERP experiments. In T. C. Handy (Ed.), *Event-Related Potentials: A Methods Handbook* (pp. 17–32). MIT Press.

Luck, S. J. (2014). *An Introduction to the Event-Related Potential Technique*. MIT Press.

Machielsen, W. C., Rombouts, S. A., Barkhof, F., Scheltens, P., & Witter, M. P. (2000). FMRI of visual encoding: Reproducibility of activation. *Human Brain Mapping*, *9*(3), 156–164. https://doi.org/10.1002/(sici)1097-0193(200003)9:3<156::aid-hbm4>3.0.co;2-q

Maris, E., & Oostenveld, R. (2007). Nonparametric statistical testing of EEG- and MEG-data. *Journal of Neuroscience Methods*, *164*(1), 177–190. https://doi.org/10.1016/j.jneumeth.2007.03.024

Mathewson, K. E., Lleras, A., Beck, D. M., Fabiani, M., Ro, T., & Gratton, G. (2011). Pulsed out of awareness: EEG alpha oscillations represent a pulsed-inhibition of ongoing cortical processing. *Frontiers in Psychology*, *2*, 99. https://doi.org/10.3389/fpsyg.2011.00099

Mazaheri, A., van Schouwenburg, M. R., Dimitrijevic, A., Denys, D., Cools, R., & Jensen, O. (2014). Region-specific modulations in oscillatory alpha activity serve to facilitate processing in the visual and auditory modalities. *NeuroImage*, *87*, 356–362. https://doi.org/10.1016/j.neuroimage.2013.10.052

Menon, G. J., Rahman, I., Menon, S. J., & Dutton, G. N. (2003). Complex visual hallucinations in the visually impaired: The Charles Bonnet syndrome. *Survey of Ophthalmology*, *48*(1), 58–72. https://doi.org/10.1016/S0039-6257(02)00414-9

Mensen, A., & Khatami, R. (2013). Advanced EEG analysis using threshold-free cluster-enhancement and non-parametric statistics. *NeuroImage*, *67*, 111–118.

Monti, M. M. (2011). Statistical analysis of fMRI time-series: A critical review of the GLM approach. *Frontiers in Human Neuroscience*, *5*. https://doi.org/10.3389/fnhum.2011.00028

Morgan, H. M., Klein, C., Boehm, S. G., Shapiro, K. L., & Linden, D. E. (2008). Working memory load for faces modulates P300, N170, and N250r. *Journal of Cognitive Neuroscience*, *20*(6), 989-1002.

Palmer, S. E. (1999). *Vision science*: *Photons to phenomenology*. MIT press.

Pearson, J., Naselaris, T., Holmes, E. A., & Kosslyn, S. M. (2015). Mental imagery: Functional mechanisms and clinical applications. *Trends in Cognitive Sciences*, *19*(10), 590–602. https://doi.org/10.1016/j.tics.2015.08.003

Pellegrini, F., Delorme, A., Nikulin, V., & Haufe, S. (2023). Identifying good practices for detecting inter-regional linear functional connectivity from EEG. *NeuroImage*, 120218. https://doi.org/10.1016/j.neuroimage.2023.120218

Pernet, C. R., Latinus, M., Nichols, T. E., & Rousselet, G. A. (2015). Cluster-based computational methods for mass univariate analyses of event-related brain potentials/fields: A simulation study. *Journal of Neuroscience Methods*. https://doi.org/10.1016/j.jneumeth.2014.08.003

Perrin, F., Pernier, J., Bertrand, O., & Echallier, J. F. (1989). Spherical splines for scalp potential and current density mapping. *Electroencephalography and Clinical Neurophysiology*, *72*(2), 184–187.

Pion-Tonachini, L., Kreutz-Delgado, K., & Makeig, S. (2019). The ICLabel dataset of electroencephalographic (EEG) independent component (IC) features. *Data in Brief*, *25*. https://doi.org/10.1016/j.dib.2019.104101

Polich, J. (2007). Updating P300: An integrative theory of P3a and P3b. *Clinical Neurophysiology*, *118*(10), 2128–2148.

Shine, J. M., Koyejo, O., Bell, P. T., Gorgolewski, K. J., Gilat, M., & Poldrack, R. A. (2015). Estimation of dynamic functional connectivity using multiplication of temporal derivatives. *NeuroImage*, *122*, 399–407.

Silani, G., Lamm, C., Ruff, C. C., & Singer, T. (2013). Right supramarginal gyrus is crucial to overcome emotional egocentricity bias in social judgments. *Journal of Neuroscience*, *33*(39), 15466–15476. https://doi.org/10.1523/JNEUROSCI.1488-13.2013

Spagna, A., Hajhajate, D., Liu, J., & Bartolomeo, P. (2021). Visual mental imagery engages the left fusiform gyrus, but not the early visual cortex: A meta-analysis of neuroimaging evidence. *Neuroscience & Biobehavioral Reviews*, *122*, 201–217.

Teunisse, R. J., Zitman, F. G., Cruysberg, J. R. M., Hoefnagels, W. H. L., & Verbeek, A. L. M. (1996). Visual hallucinations in psychologically normal people: Charles Bonnet's syndrome. *The Lancet*, *347*(9004), 794–797. https://doi.org/10.1016/S0140-6736(96)90869-7

Vanni, S., Tanskanen, T., Seppä, M., Uutela, K., & Hari, R. (2001). Coinciding early activation of the human primary visual cortex and anteromedial cuneus. *Proceedings of the National Academy of Sciences*, *98*(5), 2776–2780. https://doi.org/10.1073/pnas.041600898

Varela, F., Lachaux, J. P., Rodriguez, E., & Martinerie, J. (2001). The brainweb: Phase synchronization and large-scale integration. *Nature Reviews Neuroscience*, *2*(4), 229–239. https://doi.org/10.1038/35067550

Vogel, E. K., & Luck, S. J. (2000). The visual N1 component as an index of a discrimination process. *Psychophysiology*, *37*(2), 190–203.

Wandell, B. A., Dumoulin, S. O., & Brewer, A. A. (2007). Visual field maps in human cortex. *Neuron*, *56*(2), 366–383. https://doi.org/10.1016/j.neuron.2007.10.012

Wolpert, D. M., Goodbody, S. J., & Husain, M. (1998). Maintaining internal representations: The role of the human superior parietal lobe. *Nature Neuroscience*, *1*(6), 529–533. https://doi.org/10.1038/2245

Yao, D. (2001). A method to standardize a reference of scalp EEG recordings to a point at infinity. *Physiological Measurement*, *22*(4), 693–711. https://doi.org/10.1088/0967-3334/22/4/305

Yao, D., Wang, L., Oostenveld, R., Nielsen, K. D., Arendt-Nielsen, L., & Chen, A. C. N. (2005). A comparative study of different references for EEG spectral mapping: The issue of the neutral reference and the use of the infinity reference. *Physiological Measurement*, *26*(3), 173–184. https://doi.org/10.1088/0967-3334/26/3/003

Yuen, K. (1974). The two-sample trimmed t for unequal population variances. *Biometrika*, *61*(1), 165–170. https://doi.org/10.1093/biomet/61.1.165

Zeman, A., Milton, F., Della Sala, S., Dewar, M., Frayling, T., Gaddum, J., Hattersley, A., Heuerman-Williamson, B., Jones, K., & MacKisack, M. (2020). Phantasia–the psychological significance of lifelong visual imagery vividness extremes. *Cortex*, *130*, 426–440.

Zeman, A. Z., Dewar, M. T., & Della Sala, S. (2016). Reflections on aphantasia. *Cortex*, *74*, 336–337.

Supplement

EEG Processing – Detailed Methods

EEG data were imported into EEGLAB software 2023.0 (Delorme & Makeig, 2004) running in MATLAB R2023b and downsampled to 256 Hz. Auxiliary unused channels were removed, and scalp electrode locations were loaded using the boundary element model (BEM) spherical coordinates. Low-frequency drifts and high-frequency noise were removed using a bandpass non-causal zero-phase FIR filter (-6 dB at cut-off frequencies 0.5-45.5 Hz; filter order = 846; transition bandwidth = 1 Hz). To increase spatial resolution, data were re-referenced to infinity using the reference electrode standardization technique (REST) using the default head model (Yao, 2001; Yao et al., 2005). Abnormal channels were automatically rejected by the *clean_rawdata* plugin (default parameters) and interpolated using spherical splines (Perrin et al., 1989). On average, 0.5 (*SD* = 0.6) channels were removed across the four files (2 sessions over two separate days and two runs per day). Data were segmented from -0.5 s to +29 s around the markers indicating the beginning of each condition. Root mean square (RMS) amplitude of raw signals and a signal-to-noise ratio (SNR) metric were calculated for each trial, and outliers (i.e., trials with large amplitude or high-frequency artifacts) were detected automatically and removed using MATLAB's *isoutlier* function (*'mean'* algorithm). On average, 6.8 (*SD* = 1.3) trials were removed across the four files. In summary, after cleaning, run 1 contained 48 VMI trials and 43 *Upsight* trials; run 2 contained 46 VMI trials and 47 *Upsight* trials; run 3 contained 46 VMI and 47 *Upsight* trials; Run 4 contained 46 VMI and 49 *Upsight* trials; Session 1 (run 1 and 2 combined) contained 94 VMI and 90 *Upsight* trials and Session 2 (run 3 and 4 combined) contained 92 VMI and 96 *Upsight* trials. In total there were 370 trials analyzed, 185 VMI and 185 *Upsight*.

Blind source separation was performed using the preconditioned independent component analysis for real data (PICARD) plugin v1.0. (maximum iterations = 500; Ablin et al., 2018) with PCA-dimension reduction to account for effective data rank (Kim et al., 2023). Artifactual components were automatically classified and extracted from the EEG signals using the ICLabel plugin v1.4 (90% confidence for ocular, 95% confidence for muscular, and 99% confidence for cardiac and noise components; Pion-Tonachini et al., 2019). On average, 2.5 (*SD* = 0.6) non-brain components were rejected across the four files. Finally, the four files were merged into one for statistical analysis.

Journal of Anomalous Experience and Cognition (JAEX) 2025, Vol. 5, No. 2, pp. 136-167

For source localization and reconstruction, EEG data were downsampled to 100 Hz and segmented into 2-s epochs (requirements for the *ROIconnect* plugin). Then, the EEGLAB *ROIconnect* plugin (Pellegrini et al., 2023) was used to compute the lead field matrix (modeling the relation between the source locations and orientations of potential sources in the brain and the actual measurements made with the EEG electrodes), convert it to the Montreal Neurological Institute (MNI) coordinate system, and perform source localization and reconstruction using linearly constrained minimum variance (LCMV) beamforming. The Colin24 atlas was used to provide a parcellation scheme that assigns anatomical brain regions to the estimated neural sources (68 brain regions; see Pellegrini et al., 2023, for more details on these methods).

Source data were converted to 30-s continuous epochs (trial data) to compute the PSD on each voxel since they had to be segmented into 2-s epochs for the source reconstruction. For both the scalp and source data, PSD was computed using the Welch method on each 30-s trial using 2-s hamming windows with 50% overlap and normalized to decibels (dB).

Undirected phase-to-phase functional connectivity (FC) was computed using the multivariate interaction measure (MIM) on the source-reconstructed signals using the ROIconnect EEGLAB plugin, at the peak frequency of the effect observed in scalp and source power analyses to reduce computational cost (see Pellegrini et al., 2023, for more details on these methods).

Figure S1

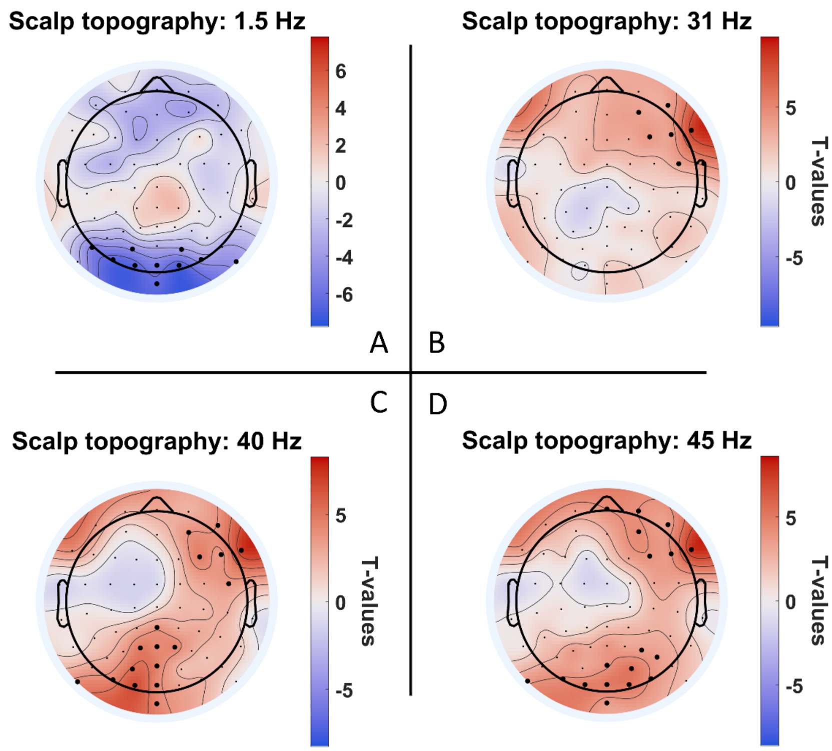

Note: Scalp topographies of the 4 other significant clusters observed in the scalp analysis (Fig. 3), depicting the cluster differences between ***Upsight*** minus visual mental imagery (VMI). **A)** Scalp distribution of the cluster's peak difference at 1.5 Hz. **B)** Scalp distribution of the cluster's peak difference at 31 Hz. **C)** Scalp distribution of the cluster's peak difference at 40 Hz. **D)** Scalp distribution of the cluster's peak difference at 45 Hz.

Étude des Processus Cérébraux Sous-Jacents à une Expérience Visuelle Inhabituelle : Une Etude de Cas

Cedric Cannard Cassandra Vieten Garret Yount Mateo Vega Fadi Kayale Arnaud Delorme

Résumé: *Contexte*. Cette étude de cas a examiné les corrélats neuronaux d'une expérience visuelle inhabituelle dans laquelle un individu perçoit en permanence des images holographiques très détaillées superposées à son champ visuel et qu'il peut partiellement moduler. Nous avons nommé cette expérience « Upsight ». Notre objectif était d'évaluer en quoi ce phénomène se rapproche ou diffère de l'imagerie mentale visuelle (IMV, comme l'hyperphantasie), de l'imagination ou des hallucinations visuelles (ex. syndrome de Charles Bonnet). *Méthode*. Des données EEG (64 canaux) ont été collectées pendant que le participant alternait entre des essais de 30 secondes en condition Upsight et en condition d'IMV (200 essais chacun). Nous avons réalisé des analyses de densité spectrale de puissance (au niveau du cuir chevelu et des

2025, Vol. 5, No. 2, pp. 136-167
Journal of Anomalous Experience and Cognition (JAEX)

niveaux de source) ainsi que des analyses de connectivité fonctionnelle (CF) des sources, et avons utilisé des statistiques robustes pour tester l'hypothèse nulle d'une absence de différence (statistiques non paramétriques et corrections de clusters spatio-temporels). *Résultats*. Les résultats au niveau du cuir chevelu ont révélé que, par rapport à la VMI, l'expérience Upsight était caractérisée par une forte diminution des puissances alpha et delta (répandue avec un pic dans les régions postérieures) et une augmentation de la puissance gamma (29-45 Hz) dans les régions frontales droites et postérieures gauches, ce qui confirme une implication accrue des processus cognitifs et visuels. De même, après la localisation de la source, nous avons observé une forte diminution de la puissance spectrale et de la CF dans la bande de fréquence alpha, dans les zones du cerveau impliquées dans le traitement visuel, l'orientation spatiale et l'intégration sensorielle, reflétant une activation corticale accrue de ces zones et des réseaux cérébraux. *Conclusions* : Upsight implique un engagement et un traitement accrus dans les réseaux visuels et cognitifs par rapport à l'IMV. Nous discutons de la phénoménologie et des résultats en relation avec l'IMV, l'imagination et les hallucinations visuelles.

French translation by Antoine Bioy, Ph. D.

Zur Untersuchung von Gehirnprozessen, die einer ungewöhnlichen visuellen Erfahrung zugrundeliegen: Eine Fallstudie

Cedric Cannard Cassandra Vieten Garret Yount Mateo Vega
Fadi Kayale Arnaud Delorme

Zusammenfassung: *Hintergrund.* Diese Fallstudie untersuchte die neuronalen Korrelate einer ungewöhnlichen visuellen Erfahrung, bei der eine Person ständig hochdetaillierte holografische Bilder wahrnimmt, die sich über ihr Gesichtsfeld legen und die sie bis zu einem gewissen Grad modulieren kann. Wir haben diese Erfahrung „Upsight" genannt. Unser Ziel war es, zu beurteilen, inwiefern dieses Phänomen mit visuellen mentalen Bildern (VMI wie Hyperphantasie), Vorstellungskraft oder visuellen Halluzinationen (z. B. Charles-Bonnet-Syndrom) zusammenhängt oder sich davon unterscheidet. *Methode*: EEG-Daten (64 Kanäle) wurden gesammelt, während der Teilnehmer abwechselnd 30-sekündige Versuche mit Upsight und visuellen mentalen Bildern (VMI) durchführte (jeweils 200 Versuche). Wir führten Analysen der spektralen Leistungsdichte (Kopfhaut- und Quellenpegel) sowie der funktionellen Konnektivität (FC) der Quellen durch und verwendeten robuste Statistiken, um die Nullhypothese der Abwesenheit eines Unterschieds zu testen (nichtparametrische Statistiken und räumlich-zeitliche Clusterkorrekturen).

Ergebnisse: Die Ergebnisse der Kopfhautmessungen zeigten, dass im Vergleich zu VMI die Upsight-Erfahrung durch einen starken Rückgang der Alpha- und Delta-Leistung (weit verbreitet mit einem Höhepunkt in den hinteren Regionen) und einen Anstieg der Gamma-Leistung (29–45 Hz) in den rechten frontalen und linken hinteren Regionen gekennzeichnet war, was eine verstärkte Beteiligung kognitiver und visueller Prozesse unterstützt. In ähnlicher Weise beobachteten wir nach der Quellenlokalisierung einen starken Rückgang sowohl der spektralen Aktivität als auch der FC im Alpha-Frequenzband in den Gehirnbereichen, die an der visuellen Verarbeitung, der räumlichen Orientierung und der sensorischen Integration beteiligt sind, was eine erhöhte kortikale Aktivierung dieser Bereiche und Gehirnnetzwerke widerspiegelt. *Schlussfolgerung*: Upsight beinhaltet im Vergleich zu VMI eine erhöhte Aktivität und Verarbeitung in visuellen und kognitiven Netzwerken. Wir diskutieren die Phänomenologie und die Ergebnisse in Bezug auf VMI, Vorstellungskraft und visuelle Halluzinationen.

German translation by Eberhard Bauer, Ph. D.

Investigando os Processos Cerebrais Subjacentes a uma Experiência Visual Incomum: Um Estudo de Caso

Cedric Cannard Cassandra Vieten Garret Yount Mateo Vega
Fadi Kayale Arnaud Delorme

Resumo: *Contexto*. Este estudo de caso investigou os correlatos neurais de uma experiência visual incomum na qual um indivíduo percebe constantemente imagens holográficas altamente detalhadas sobrepostas em seu campo visual e pode modulá-las até certo ponto. Chamamos essa experiência de Upsight. Nosso objetivo foi avaliar como o fenômeno pode se relacionar ou diferir de imagens mentais visuais (VMI, como hiperfantasia), imaginação ou alucinações visuais (por exemplo, Síndrome de Charles Bonnet). *Método*: Os dados do EEG (64 canais) foram coletados enquanto o participante alternava entre tentativas de 30 segundos em condições de Upsight e imagens mentais visuais (VMI) (200 tentativas cada). Realizamos análises de densidade espectral de potência (nos níveis de escalpo e fonte), bem como análises de conectividade funcional da fonte (FC), e estatísticas robustas para testar a hipótese nula de ausência de diferença (estatísticas não paramétricas e correções de agrupamento espaço-temporal). *Resultados*: Os resultados do escalpo revelaram que, em relação ao VMI, a experiência do Upsight foi caracterizada por fortes diminuições de potência alfa e delta (generalizadas com pico nas regiões posteriores) e aumento da potência gama (29-45 Hz) nas regiões frontal direita e posterior esquerda, apoiando o aumento do envolvimento dos processos cognitivos e visuais. Da mesma forma, após a localização da fonte, observamos uma forte diminuição na potência espectral e FC na banda de frequência alfa, em áreas cerebrais envolvidas no processamento visual, orientação espacial e integração sensorial, refletindo o aumento da ativação cortical dessas áreas e redes cerebrais. *Conclusões*: Upsight envolve maior envolvimento e processamento em redesvisuais e cognitivas em relação ao VMI. Discutimos a fenomenologia e os resultados em relação ao VMI, imaginação e alucinações visuais.

Portuguese translation by Antônio Lima, Ph. D.

Journal of Anomalous Experience and Cognition (JAEX) 2025, Vol. 5, No. 2, pp. 136-167

Un Estudio Sobre los Procesos Cerebrales Subyacentes a una Experiencia Visual Inusual: Un Estudio de Caso

Cedric Cannard   Cassandra Vieten   Garret Yount   Mateo Vega
Fadi Kayale   Arnaud Delorme

Resumen: *Antecedentes*. Este estudio de caso investigó los correlatos neurales de una experiencia visual inusual en la que un individuo percibe constantemente imágenes holográficas muy detalladas superpuestas en su campo visual y puede modularlas parcialmente. Denominamos a esta experiencia *Upsight*. Nuestro objetivo fue evaluar cómo el fenómeno es semejante o difiere de las imágenes mentales visuales (IMV, como la hiperfantasia), la imaginación, y las alucinaciones visuales (por ejemplo, el síndrome de Charles Bonnet). *Método*: Obtuvimos datos de EEG (64 canales) mientras el participante alternaba entre muestras de 30 segundos de Upsight e imágenes mentales visuales (VMI) (200 muestras de cada una). Analizamos la densidad de poder espectral (a niveles de cuero cabelludo y fuente) y de conectividad funcional (CF) de la fuente, utilizando estadísticas robustas para evaluar la hipótesis nula de no diferencia (estadísticas no paramétricas y correcciones de conglomerados espaciotemporales). *Resultados*: Los resultados a nivel de cuero cabelludo revelaron que, en contraste con IMV, Upsight se caracterizó por fuertes disminuciones de poder alfa y delta (generalizada con un pico en las regiones posteriores), y un aumento del poder gamma (29-45 Hz) en las regiones frontal derecha y posterior izquierda, lo que apoya una mayor involucración de procesos cognitivos y visuales. Así mismo, tras la localización de la fuente, observamos una fuerte disminución tanto en el poder espectral como en la CF en frecuencia alfa, en áreas cerebrales implicadas en procesamiento visual, orientación espacial, e integración sensorial, lo que refleja una mayor activación cortical de estas áreas y redes cerebrales. *Conclusiones*: El Upsight implica una mayor involucración y procesamiento de las redes visuales y cognitivas en comparación con el IMV. Discutimos la fenomenología y los resultados en relación con el IMV, la imaginación, y las alucinaciones visuales.

Spanish translation by Etzel Cardeña, Ph. D.